Topic: EX-S

Observation of a resistive wall and ferritic wall modes in a line-tied, screw pinch with a rotating conducting wall

C. Paz-Soldan[1], W.F. Bergerson[2], M. Brookhart[1], G. Fiksel[3], D. Hannum[1], C. Hegna[1], and J.S. Sarff[1], C.B. Forest[1]

1) University of Wisconsin, Madison, Wisconsin, and the Center for Magnetic Self-Organization in Laboratory and Astrophysical Plasmas
2) The University of California at Los Angeles, Los Angeles, California
3) University of Rochester, Rochester, New York

E-mail contact: cbforest@wisc.edu

We report an overview of theoretical and experimental results from research on the Rotating Wall Machine, a linear screw pinch experiment at the University of Wisconsin. The overall goal of the work is to test the hypothesis that moving metal walls can stabilize the resistive wall mode (RWM) in the simplified (relative to a torus) geometry of a cylinder where spinning, solid conducting walls can be used instead of flowing liquid metals.

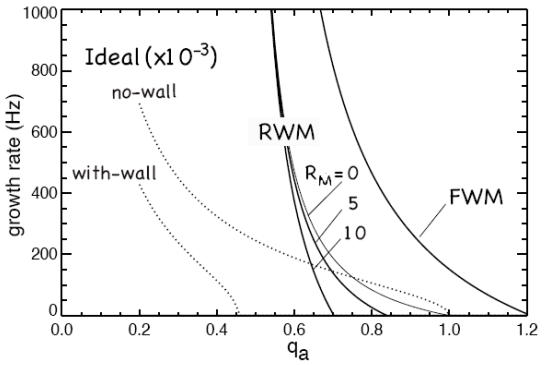

Figure 1: Growth rates predicted for ideal modes and RWMs with a rotating shell in a line tied pinch. The plasma radius a=7.5 cm, the stationary first wall radius b=10 cm, and spinning second wall radius c=12 cm. The wall time $\tau_b \sim \tau_c = \mu\sigma\delta_b b \approx 10$ ms and $R_m=\omega_c\tau_c$ is shown for three different rotation rates. Also shown is the Ferritic Wall Mode (FWM) is the RWM with stationary shells and μ=50.

Theory. The growth rates for the RWM in a line-tied screw pinch with rotating walls has been theoretically derived [1] and is summarized in Fig. 1 where the growth rates for the ideal with-wall (perfect wall), ideal no-wall, and RWMs are shown for the experiment. An ideal stationary wall of radius *b* surrounding a plasma of radius *a* modifies the Kruskal-Shafranov condition to give a stability window for current driven kink modes of $1-(a/b)^2 < q_a < 1$; finite wall resistivity allows the RWM to grow on the wall time in this region. When two shells are used, with one shell rotating, the RWM can be stabilized for sufficiently high rotation speeds of the second shell. Interestingly, when the second wall is ferromagnetic, the external kink can be destabilized for $q_a>1$ and this variant of the RWM is known as the Ferritic Wall Mode (FWM).

Device. The experiment [2], shown in Fig. 2, is a 1.2 m long, 0.2 m diameter, line-tied screw pinch utilizing a solenoidal field of up to 1 kG. Line-tying is provided by thick copper plates at each end of the machine whose characteristic resistive diffusion time is much longer than the discharge duration. Plasma is created by discharging an array of electrostatic plasma guns, inside each of which high density plasma allows for large space-charge limited currents to be sourced when the plasma gun is biased relative to an external anode. Each gun in the array is independently biased and utilizes a pulse-width modulation system to precisely control the injected current waveform. The gun array thus allows for controllable current density profiles in both space and time. The central column is interchangeable allowing a variety of vacuum vessel walls and liners to be installed. Experiments have been conducted with insulating (Pyrex), conducting (SS304, copper), and magnetic (mu-metal) boundary conditions. A rotating wall has also been constructed which rotates relative to the stationary central column at speeds of up to 280 km/h, corresponding to a magnetic Reynolds number of 5.

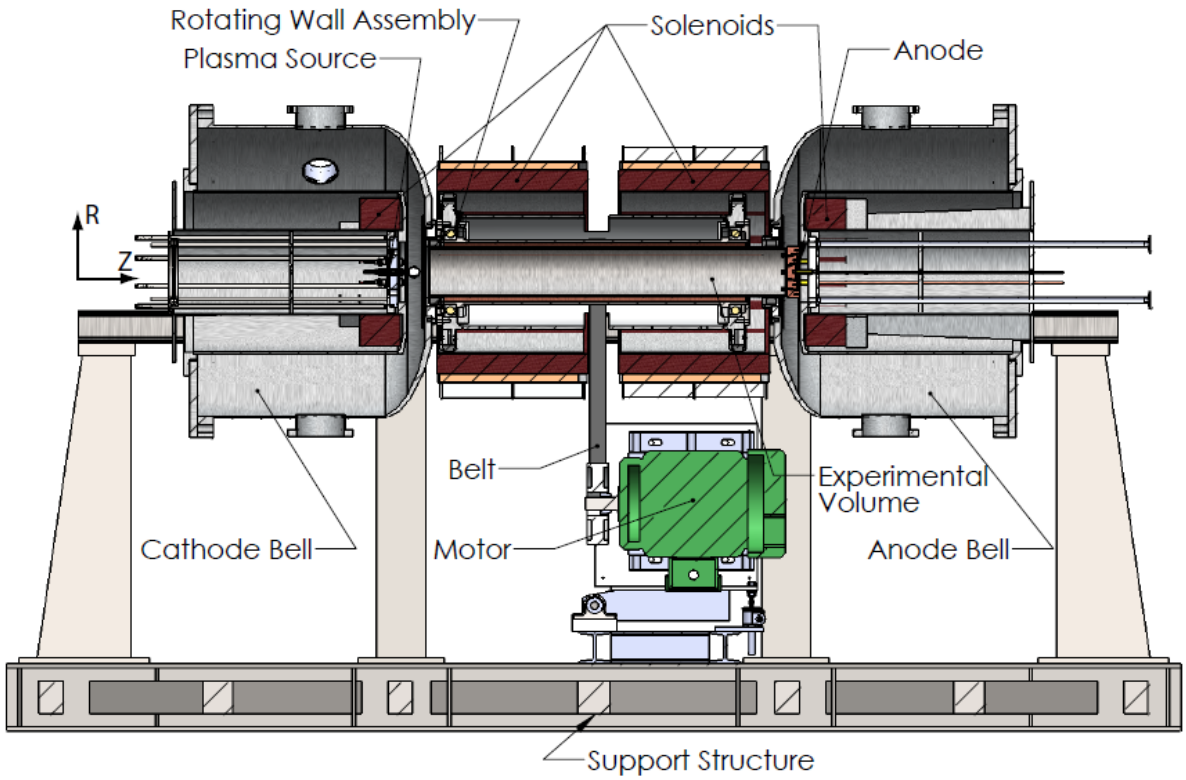

Figure 2: Cross Section of the Rotating Wall Machine: The plasma is generated at the plasma source array and is confined by four solenoids. Biasing the source with respect to the anode drives current throughout the discharge and excites current-driven instabilities. The plasma is surrounded by a static vacuum vessel wall around which the rotating wall spins.

Plasma Characterization. Probes have been used to measure axial and radial profiles of magnetic field, current density, electron density, temperature, and plasma potential. These measurements have also been used to estimate particle diffusion and radial current. The plasma source is very high density ($n>2\times10^{20}$ m^{-3}) and provides an axially flowing plasma that diffuses radially. Radial transport is ambipolar: the density is a plume that broadens as it flows out from the guns, but the current profile is tightly collimated. The measured potential drop required for driving the axial current along the column results in sheared azimuthal ExB rotation in which the cathode end of the plasma is spinning rapidly, but the anode end is nearly stationary, as shown in Fig. 3.

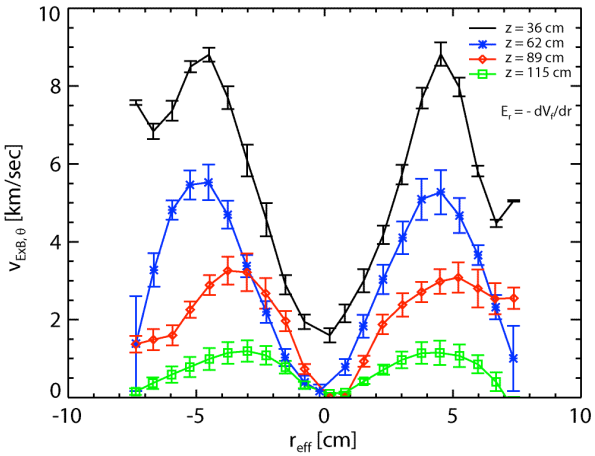

Figure 3: Inferred ExB velocity profiles using floating potential profiles taken by a single-tip Langmuir probe. The electrostatic fields arise from the high bias voltages (100V) applied across the device to drive large currents (1kA). The inferred flow is heavily sheared in both the radial and axial direction.

Magnetic probes indicate that the plasma is strongly diamagnetic during low plasma (bias) current discharges, as shown in Fig 4. (left). Heating from the plasma gun array produces high density plasma whose pressure gradient is supported by diamagnetic currents. The highly conducting anode suppresses these diamagnetic currents resulting in a modest magnetic mirror at the anode end. As the plasma current is increased, larger parallel currents give rise to a transition to core paramagnetism, as shown in Fig. 4.b. Increasing the plasma current also initiates the transition from a stable to unstable plasma as the discharge begins to exhibit high-

frequency (~10 kHz) ideal and low frequency (~0Hz) resistive instabilities. Internal measurements of the current density profiles also show the coalescence of the individual current channels into an axisymmetric current profile as a result of magnetic shear, phase mixing, and diffusion.

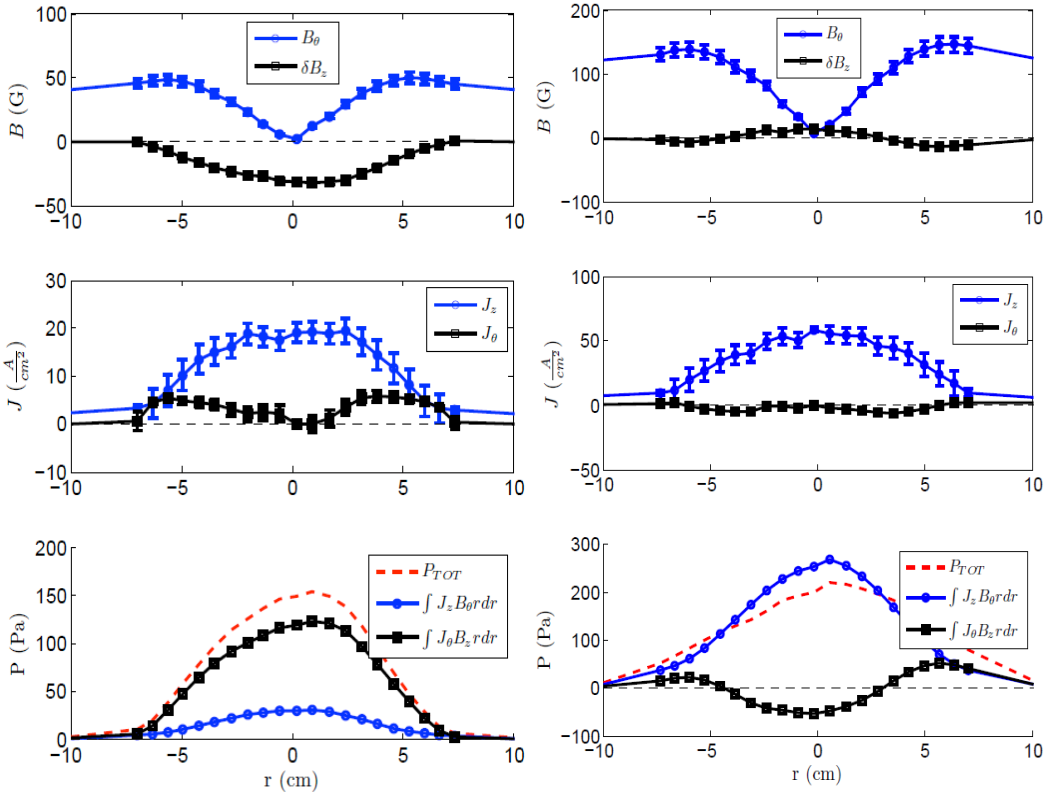

Figure 4: Equilibrium currents and magnetic fields as measured by a magnetic probe indicates that the plasma in the device is strongly diamagnetic at low currents (left). At large plasma current (right), the discharge becomes paramagnetic in the core.

Experimental observation of the RWM and FWM. Recent work has lead [3] to a clear identification of the resistive wall mode in the experiment; electrically thin, thick, and ferritic shells have been used on the device and an external kink mode has been observed. The growth rate of this mode scales inversely with the shell resistive diffusion time as shown in Fig. 2. The FWM was also identified in the device. Discharges in which a mu-metal shell (in addition to the thick copper shell) surrounded the plasma were found to be significantly destabilized to the external kink. The plasma is stable without the mu-metal and destabilized with it for $q_a > 1$. Furthermore, the growth rate of the FWM was found to be significantly larger than expected by theory.

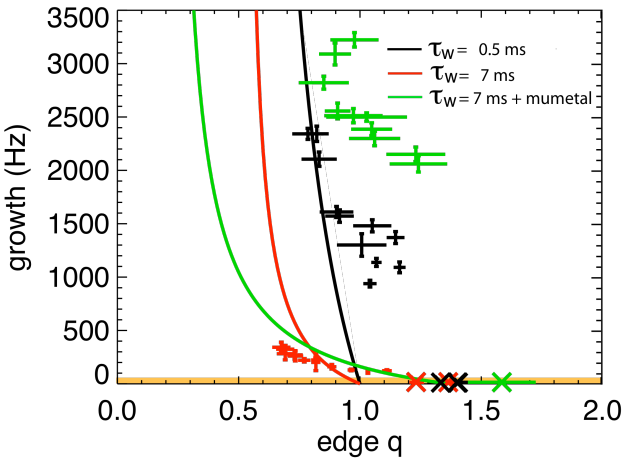

Figure 5: Measured (data) and predicted growth (lines) rates for the FWM and RWM in a line-tied pinch. The black and red lines correspond to the theoretical predictions for the RWM with purely resistive walls while the green line corresponds to the FWM. Stable plasmas are marked by crosses.

Interaction of the RWM with a Rotating Wall: Recent experiments have demonstrated the stabilization of the RWM by a rotating solid conducting wall surrounding the plasma. Additionally, a strong dependence of RWM stabilization on rotating wall speed and direction has been observed, shown in Fig. 6. RWM mode amplitudes near the end of the discharge duration illustrate a clear scaling with wall speed. In the positive direction (arbitrary convention), the rotating wall is destabilizing, while in the negative direction the wall is strongly stabilizing. This dataset was collected under a constant current profile with an edge safety factor q_a of 0.87. The observed asymmetry in rotation is not captured in the present theory, and it suggests that an intrinsic azimuthal flow in the plasma results in different apparent wall rotation velocities in the frame of the spinning plasma.

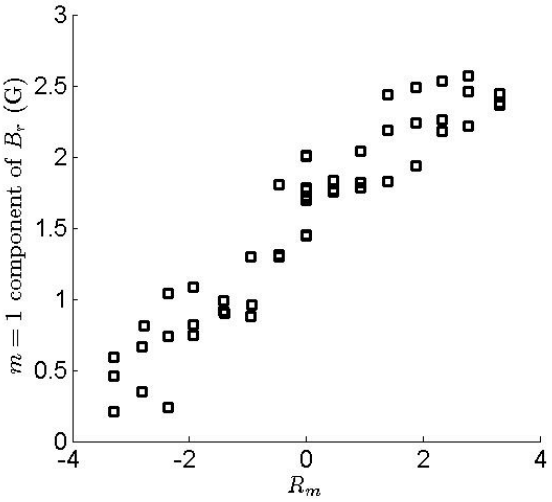

Figure 6: The amplitude of the m=1 component of the Br field is strongly dependent on the speed and direction of the rotating wall. Strong asymmetry is seen between forward and reverse (arbitrary convention) wall rotation.

The RWM eigenfunction in the static wall (shown in Fig. 7, middle) illustrates a well developed mode with an observable pitch along the axial length of the machine. The forward rotation RWM eigenfunction (Fig. 7, top) is both larger in amplitude and shifted azimuthally in the direction of the wall rotation. The reverse rotation case (bottom) is drastically different: for most of the length of the device the mode has been stabilized. Near the plasma gun (z=0 cm), a perturbation is present and it has also been shifted azimuthally in the direction of wall rotation. Probe measurements have indicated that the region near the guns is dominated by flux-rope merger dynamics. It is believed that this process may interfere with the stabilization process.

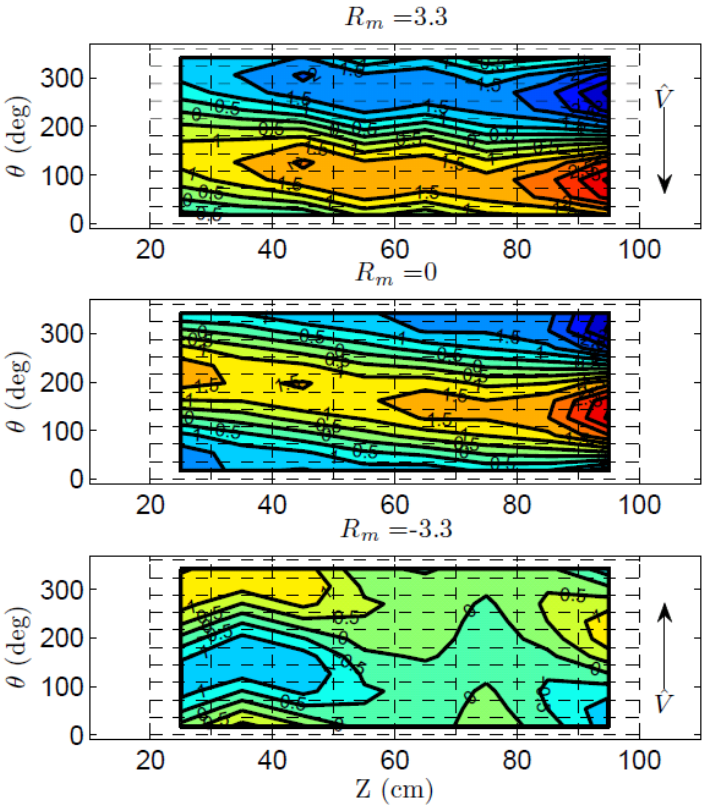

Figure 7: Contour plots of the m=1 component of B_r as measured by a flux-loop array surrounding the plasma (shown by dashed lines). The mode is seen to only be suppressed in one direction of wall rotation. The location of the mode is also affected by rotation, with positive (negative) convention wall velocity rotating the mode through negative (positive) azimuthal angle.

Evolutions of the mode in time (shown in Fig. 8) for the cases illustrated above support the same conclusions. For the static wall case, the RWM is seen to grow up from a small error field at t=6ms, after which time the mode grows first through its linear phase and then slows as it enters a non-linear phase characterized by slower growth. For both of these phases the mode is locked to the static wall. The forward rotation case is clearly less stable, with both a larger linear phase growth rate and final

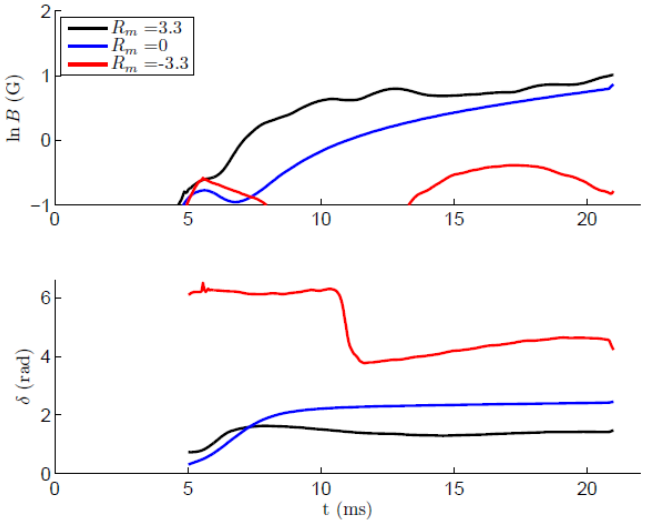

Figure 8: The m=1 component of the Br field as measured by ring of flux-loops at a single axial location demonstrates drastically different behavior as a function of wall rotation. The mode is effectively stabilized in the negative rotation case, while positive rotation destabilizes the mode. The static and positive rotating cases appear to be locked to the static wall during the saturation phase at the end of the discharge.

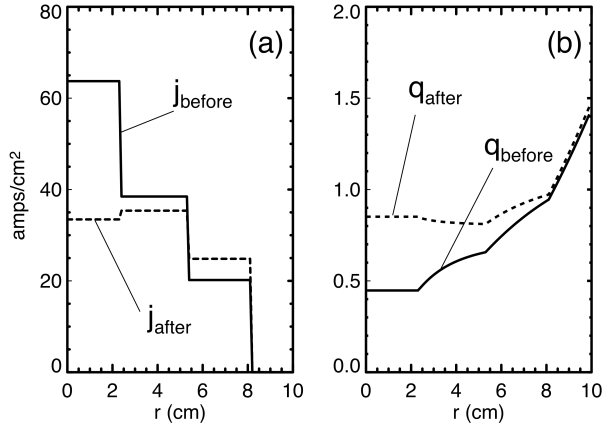

Figure 9: (a) The current density measured by a segmented anode and (b) the corresponding q profile during a discrete current relaxation event.

amplitude. The mode shows some rotation before it too locks to the static wall. In the reverse direction case the amplitude quickly decreases from the beginning of the discharge and remains below 0.5 G for the discharge duration. This case is similar to the no-plasma case, which still exhibits magnetic activity due to the advection of error field components of the axial guide field by the rotation of the conducting wall.

Line-Tied Reconnection. Finally, MHD phenomena exhibiting both ideal and resistive characteristics have been clearly observed without a nearby conducting shell. The no-wall instability begins as an ideal, line tied internal kink mode that grows and then saturates as a rotating helical structure. If the plasma current is increased further, a phenomenon reminiscent of sawtooth relaxations in tokamaks has been discovered: the current profile is observed to periodically flatten in discrete bursts of MHD activity, concurrent with topological changes in the magnetic field geometry. Both modes appear when the central value of the safety factor drop below a value of order 1 as shown in Fig. 9.

Work supported by the U.S. Department of Energy and National Science Foundation.

[1] C.C. Hegna, Phys. Plasmas **11**, 4230 (2004).
[2] W.F. Bergerson, C. B. Forest, G. Fiksel, D.A. Hannum, R. Kendrick, J.S. Sarff and S. Stambler, Phys. Rev. Lett. **96,** 015004 (2006).
[3] W.F. Bergerson, D.A. Hannum, C.C. Hegna, R. Kendrick, J.S. Sarff, and C.B. Forest, Phys. Rev. Lett. **101,** 235005 (2008).